Desalination and Water Treatment
www.deswater.com

51 (2013) 1337–1343
February

1944-3994/1944-3986
doi: 10.1080/19443994.2012.700037

Taylor & Francis
Taylor & Francis Group

Fabrication of electrospun nanofibrous membranes for membrane distillation application

L. Francis*, H. Maab, A. AlSaadi, S. Nunes, N. Ghaffour, G.L. Amy

Water Desalination and Reuse Centre, King Abdullah University of Science and Technology (KAUST), Thuwal 23955-6900, Saudi Arabia
Tel. +96 (2) 8082196; email: lijo.francis@kaust.edu.sa

Received 22 February 2012; Accepted 29 May 2012

ABSTRACT

Nanofibrous membranes of Matrimid have been successfully fabricated using an electrospinning technique under optimized conditions. Nanofibrous membranes are found to be highly hydrophobic with a high water contact angle of 130˚. Field emission scanning electron microscopy and pore size distribution analysis revealed the big pore size structure of electrospun membranes to be greater than 2 μm and the pore size distribution is found to be narrow. Flat sheet Matrimid membranes were fabricated via casting followed by phase inversion. The morphology, pore size distribution, and water contact angle were measured and compared with the electrospun membranes. Both membranes fabricated by electrospinning and phase inversion techniques were tested in a direct contact membrane distillation process. Electrospun membranes showed high water vapor flux of 56 kg/m^2-h, which is very high compared to the casted membrane as well as most of the fabricated and commercially available highly hydrophobic membranes.

Keywords: Electrospinning; Nanofibers; Membrane distillation; Water vapor flux

1. Introduction

Our world is facing a water and energy shortage. One-sixth of the world's population have no access to improved drinking water, and "All the signs suggest that it is getting worse and will continue to do so, unless corrective action is taken" [1]. Nonconventional water resources such as desalination will undoubtedly play an increasing role in meeting worldwide water needs, but it is limited by its high cost, which is largely dominated by energy costs [2]. This explains why the desalination technologies are mainly used in countries where abundant fossil fuel is available. The separation of freshwater from saltwater can be achieved in many ways and these are discussed at length in standard texts on desalination [3].

As an alternatively new process, membrane distillation (MD) is being investigated as a low cost and energy saving process using low-grade energy waste heat source compared to the conventional thermal-based and membrane-based separation processes [4–6]. MD is a thermally driven process in which water is the major component present in the feed solution to be treated. There is a thermally driven vapor transport through nonwetted porous hydrophobic membranes, where the driving force is the partial vapor pressure difference across the two sides of the membrane pores

*Corresponding author.

Presented at the International Conference on Desalination for the Environment, Clean Water and Energy, European Desalination Society, 23–26 April 2012, Barcelona, Spain

[7]. In MD process, the membrane acts only as a barrier between the two phases involving mass transfer and does not directly contributes to the process selectivity [8]; in addition, the productivity, long-term stability, and energy efficiency of the process are highly dependent on the membrane properties [7–9]. Characteristics required for a good direct contact membrane distillation (DCMD) membrane to yield high water vapor flux, long-term stability, and high energy efficiency are high hydrophobicity, optimum pore size and narrow pore size distribution, high bulk and surface porosities, high degree of pores interconnectivity, low thermal conductivity, and an optimum thickness [8,9].

Our research group has developed polymeric nanofibrous membranes with improved properties for MD desalination application. Electrospinning was employed as a technique for the fabrication of microporous nanofibrous membrane. Electrospinning is a cost effective method for the fabrication of nonwoven nanofibrous membranes having large surface to volume ratios and various fiber morphologies and geometries [10]. Researchers have used electrospun nanofibers in various potential applications such as tissue engineering [11–13], photo voltaic cells [14,15], high performance air filters [16], membranes for separation processes [17,18], sensors [19,20], advanced composites [21,22], etc. Electrospun nanofibrous membranes have properties such as high porosity and large pore size with narrow pore size distribution and large surface area. These properties are most desirable for MD process to produce high water vapor flux.

In this study, we have fabricated nanofibrous membranes of Matrimid solution via electrospinning technique. The membranes were characterized and tested in DCMD process for sea water desalination. The influence of feed solution temperature as well as permeate temperature on water vapor flux was studied. Matrimid membranes were fabricated via casting followed by phase inversion and their DCMD performance was compared with that of electrospun nanofibrous membranes.

2. Experimental

Matrimid 5218 and N-methyl pyrrolidone (NMP) were purchased from Huntsmann Advanced Materials (USA) and Sigma Aldrich, respectively. Matrimid was dissolved in NMP to obtain 18% (w/w) and was electrospun by using an electrospinning apparatus, ES 2000 (Japan). Matrimid solution was fed into a standard 5 ml glass syringe attached to a 25G blunted stainless steel needle. A 30 kV DC voltage was applied to the syringe tip and the flow rate was adjusted to 15 μL/min. Aluminum foil mounted on a rectangular metallic plate was fixed at a distance of 17 cm from the syringe tip and used as collector to collect polymeric nanofibers from the syringe. By increasing the voltage, the semispherical form of polymeric solution at the tip of the syringe needle will deform into the form of a cone (Taylor Cone) and beyond a particular voltage a fast jet of polymeric solution will eject from the apex of the Taylor cone in the form of nanofibers to the grounded collector plate. The grounded collector plate was moved in a zigzag direction to collect nanofibers uniformly throughout the spinning process. Another batch of Matrimid solution was prepared with the same concentration and electrospinning was carried out with the same spinning parameters on a polyester support mounted on a grounded collector plate to obtain composite Matrimid nanofibrous membrane. After electrospinning the resultant Matrimid nanofibrous membrane and polyester Matrimid composite membranes were pealed from the aluminum foil and kept in a vacuum oven at 60 °C for 12 h.

Eighteen percent Matrimid solution was prepared and cast on a glass plate and, using a 150 μm knife, the solution was evenly spread throughout the surface of the glass plate and immediately dipped in a water bath for 1 h to get a flat sheet Matrimid membrane via phase inversion. The membrane was dried in a vacuum oven for 12 h. All of the fabricated Matrimid membranes were subjected to different characterization techniques as well as MD testing.

Membrane samples were sputter coated using a Sputter Coater machine (EMITECH K575 X, UK) to coat a thin gold layer to make the film surface conductive. The surface morphology of polyimide nanofibers was studied under field emission scanning electron microscope (SEM; Quanta 200 FEG System: FEI Co., USA). The average fiber diameter distribution was analyzed from the SEM images using Image J analysis software. (Image J, National Institutes of Health, USA). Mean flow pore size (MFP), first bubble point (FBP), and pore size distribution were measured using a IB-FT Gm bH Porolux 1,000 Porometer (Germany) by wet-up/dry-up method and the analysis was done by using Automated Capillary Flow Porometer system software. Average pore size and pore size distribution of composite Matrimid membranes were calculated from the SEM image by using Image J analysis software. The hydrophobic nature of membranes fabricated via electrospinning and phase inversion was determined by measuring the water contact angle of membranes by using a Attension, KSV instruments T 301 (Finland). According to Young's equation [23]:

$$\gamma^{sv} = \gamma^{sl} + \gamma^{lv} \cos\theta \quad (1)$$

where γ^{sv} is the solid surface free energy, γ^{sl} is the solid/liquid interfacial free energy, γ^{lv} is the liquid surface free energy, and θ is the contact angle.

All membranes were cut into 6 × 6 cm pieces to fit into a MD module and subjected to MD testing at different optimized processing conditions using a laboratory-scale MD setup. Seawater was preheated to desired temperatures and circulated through the membrane module, whereas the pure cold water was circulated through the other side of the membrane simultaneously in counter current direction. Salt concentrations of both permeate and feed solutions were determined by using conductivity meter (Oakton Eutech Instruments, Malaysia). The salt rejection (β) and water vapor flux (J_v) were determined by the following equations:

$$\beta = \left(1 - \frac{C_p}{C_f}\right) \times 100 \quad (2)$$

$$J_v = M_w / At \quad (3)$$

where C_p and C_f are the salt concentrations of bulk permeate and feed solutions, respectively; M_w (kg) is the weight of collected permeates, A (m^2) is the effective membrane area, and t (h) is the time interval. The influence of water vapor flux on feed solution temperature over a range of 40–80˚C was studied by maintaining temperature of the permeate side at 20˚C. The influence of transmembrane flux was also studied over a range of 10–30˚C by keeping feed solution temperature constant at 60˚C.

3. Results and discussion

Fig. 1 shows the schematic diagram of an electrospinning setup.

Polymeric nanofibrous membranes were obtained from a Matrimid solution. Table 1 shows the processing parameters and conditions used for electrospinning.

Fig. 2 shows the SEM images of the nanofibrous Matrimid membrane and the membrane obtained via phase inversion. Both of the membranes show different morphologies.

Nanofibers appear to be randomly distributed and highly porous with open structure, whereas the membrane fabricated using phase inversion shows a smooth surface with many small pores. Fig. 3 shows the fiber diameter distribution of nanofibers in the electrospun membrane and reveals that the diameter distribution is narrow.

More than 75% of the fibers have a diameter in the range of 250–370 nm and the average fiber diameter

Table 1
Conditions of electrospinning

Parameters	Conditions
Concentration	18% (w/w)
Flow rate	15 µL/min
Applied potential	30 kV
Humidity	50–60%

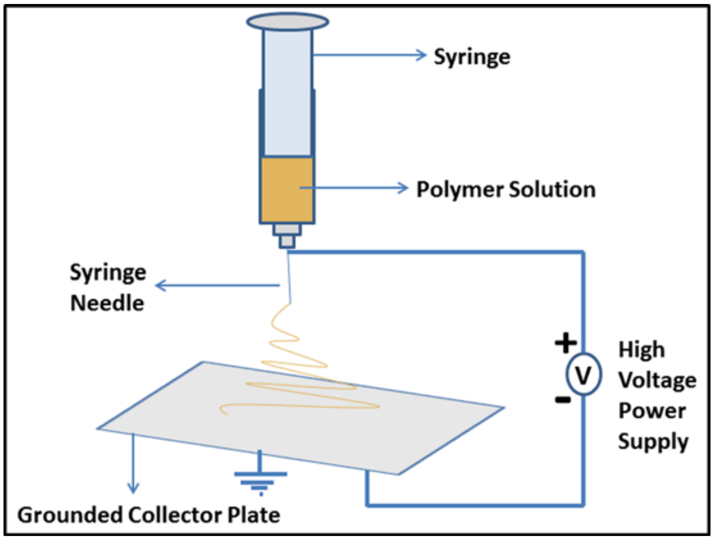

Fig. 1. Schematic diagram of electrospinning.

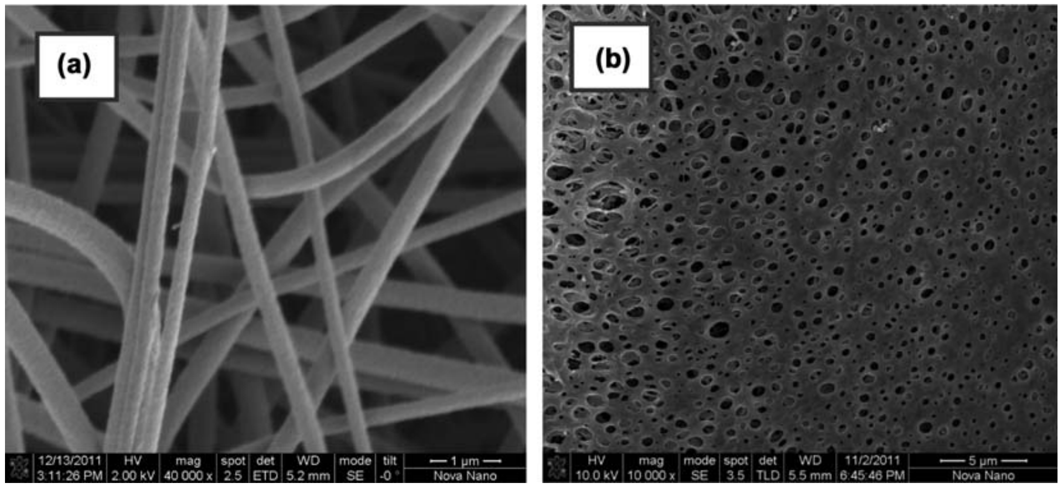

Fig. 2. SEM images of (a) electrospun nanofibrous Matrimid membrane and (b) Matrimid membrane fabricated by phase inversion.

was measured to be 290 nm. The MD process is classified as microfiltration and membrane pore size plays a very important role in the mass transport across the membrane to obtain considerable water vapor flux. Fig. 4(a) and (b) shows the pore size distribution of the electrospun Matrimid membrane and composite Matrimid membrane fabricated by phase inversion, respectively.

The MFP of the electrospun membrane was measured to be 2.15 μm, whereas that of the casted membrane was observed to be 0.2 μm. The FBP and smallest pore of electrospun membrane were measured to be 3.12 and 1.71 μm, respectively. The pore size distribution of composite Matrimid membrane was obtained from the analysis of SEM image by using Image J software. The pore size distribution was found to be narrow and more than 80% of the pores are found to have an average diameter in the range of 0.1–0.3 microns. It was found to be a tenfold increase in the average pore size of 2.15 μm of electrospun membranes. Larger pore size allows more vapors and this considerable difference in the average pore size could be the important reason for the high water vapor flux of electrospun membranes compared to the composite Matrimid membranes fabricated by phase inversion technique.

Fig. 5 shows the images taken during water contact angle measurements of different Matrimid mem-

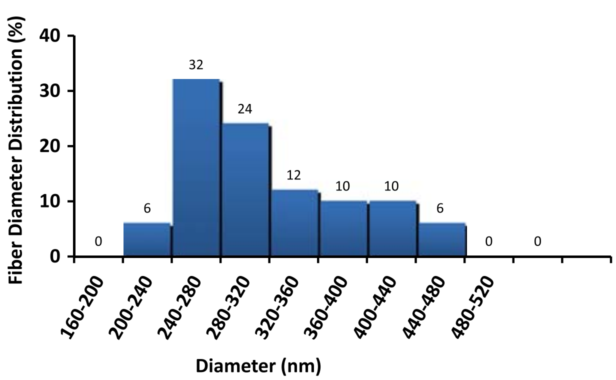

Fig. 3. Fiber diameter distribution of Matrimid nanofibers.

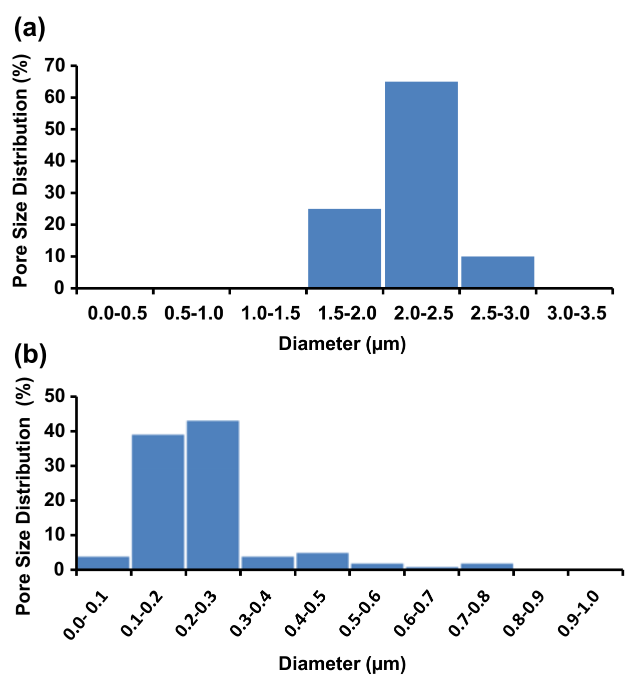

Fig. 4. Pore size distribution of (a) electrospun Matrimid nanofibrous membrane and (b) phase inversion Matrimid membrane.

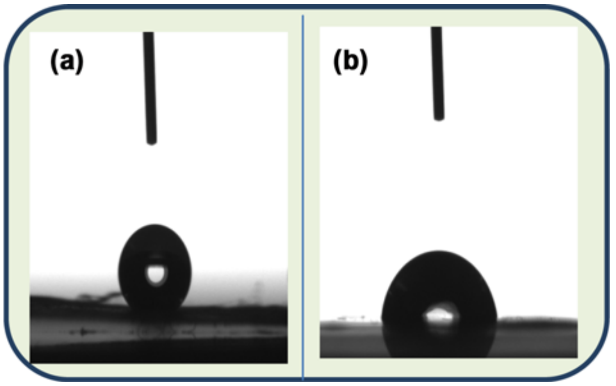

Fig. 5. Water contact angle measurements (a) electrospun membrane and (b) phase inversion membrane.

branes. The image of water droplet on electrospun membrane is more spherical than that of the composite membrane fabricated by phase inversion. Table 2 shows the results of contact angle measurements. An average of five different measurements on a membrane was taken as the water contact angle of the membrane. It was observed that the water contact angle of electrospun membrane is considerably higher than that of the membranes fabricated via phase inversion. Electrospun membranes show a water contact angle of 130.0 ± 2.2˚ whereas the casted membranes show 85 ± 1.8˚, which is 35% less than that of electrospun membranes. It is possible to obtain high surface roughness during electrospinning process due to the nanofibrous morphology; moreover, nanofibers are randomly overlaid throughout the membrane.

Table 2
Water contact angle measurements

Replicate	Electrospun membrane	Composite membrane
1	127.8	84.1
2	131.5	86.8
3	130.0	85.9
4	132.2	83.2
5	128.5	85.0
Average	130.0 ± 2.2	85.0 ± 1.8

Fig. 6 shows the schematic representation of the laboratory-scale setup of MD and Fig. 7 represents the influence of feed temperature on water vapor flux at constant permeate temperature. An increase in the feed solution temperature results in an increase in the partial vapor pressure difference between the feed and permeate side of the membrane, which results in the increase in the transmembrane flux across the membrane. It is clear that electrospun Matrimid membranes yield a higher water flux reaching 56 kg/m^2-h at 80 ℃ when compared to the composite Matrimid membranes fabricated via phase inversion, with flux of the later observed to be 24 kg/m^2-h; this is a 243% increase in the water flux for elecrospun nanofibrous membranes compared to the Matrimid membranes fabricated via phase inversion.

There is no significant deviation in the water vapor flux between the nonsupported electrospun Matrimid membrane and the composite nanofibrous Matrimid membrane obtained by electrospinning on a polyester support. High water flux shown by electrospun membranes is attributed to their highly open pore structure with a larger pore size, interconnectivity of pores, and pore size distribution of membranes compared with the membranes obtained via phase inversion. Theoretically, MD provides 100% salt

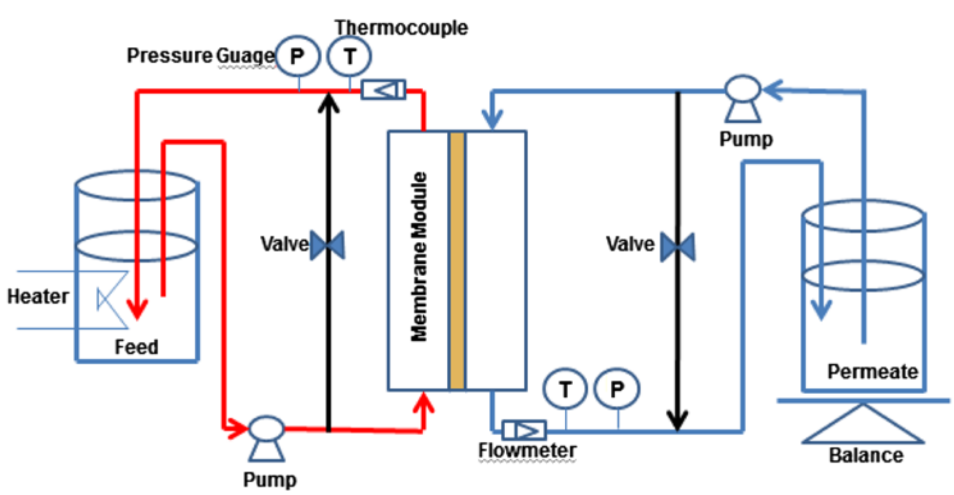

Fig. 6. Schematic representation of laboratory-scale DCMD setup.

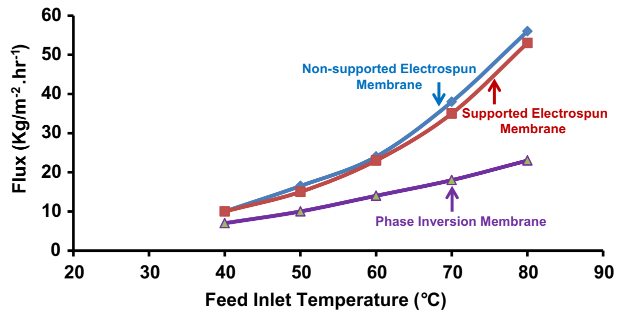

Fig. 7. Influence of feed inlet temperature on permeate flux at feed flow rate = permeate flow rate = 1 L/min and at a permeate inlet temperature of 20 ℃.

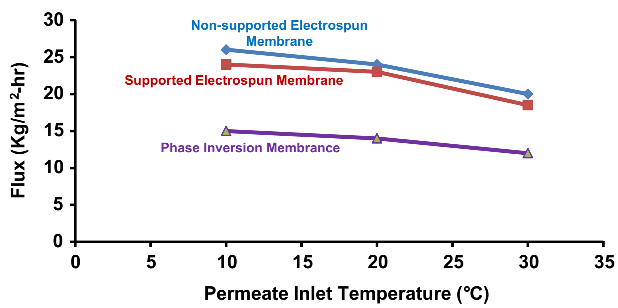

Fig. 8. Influence of permeate inlet temperature on permeate flux at feed flow rate = permeate flow rate = 1 L/min and at a feed inlet temperature of 60 ℃.

rejection because of the fact that the hydrophobic microporous membrane only allows transport of water vapors and noncondensable gasses while strictly retaining salts. In our study, all the fabricated membranes show high salt rejection of about 99.99%. While investigating the DCMD performance by changing permeate inlet temperature from 10 to 30℃ at a constant feed solution temperature of 60℃, a small decrease in water vapor flux was observed (Fig. 8). This is because the vapor pressure formation at lower temperature is less than that at higher degrees of temperatures. Fig. 8 shows the influence of permeate inlet temperature on the transmembrane flux at constant feed solution temperature as well as the constant feed and permeate flow rate for all types of fabricated membranes.

4. Conclusions

The main objective of this study was to fabricate the nanofibrous Matrimid membranes by using an electrospinning technique and testing their performance in DCMD process. The experimental results can be summarized as follows:

(1) Nanofibrous Matrimid membranes were successfully fabricated by using the electrospinning technique.
(2) Fabricated membranes showed large pore size (2.1 μm) and a pore size distribution with high interconnectivity between pores resulting in high water vapor flux with high salt rejection (99.99%).
(3) The electrospinning process helped to fabricate membranes with maximum surface roughness and it results in high water contact angle (130˚) which prevents the pore wetting and hence increase the lifetime of membranes.
(4) The DCMD performance of electrospun membranes was compared with composite Matrimid membranes fabricated via phase inversion and it was found that the former membranes show much better performance. In short, electrospinning is a reliable and promising technique for the fabrication of membranes for the MD process.

References

[1] UNESCO, The United Nations World Water Development Report—Water for People—Water for Life (Executive Summary), UNESCO Publishing, Berghahn Books, Paris, 2003.
[2] K.V. Reddy, N. Ghaffour, Overview of the cost of desalinated water and costing methodologies, Desalination 205 (2007) 340–353.
[3] K.S. Spiegler, Y.M. El-Sayed, A Desalination Primer Introductory Book for Students and Newcomers to Desalination, Balaban Desalination, Santa Maria Imbaro, 1994.
[4] M. Khayet, M.P. Godino, J.I. Mengual, Possibility of nuclear desalination through various membrane distillation configurations: a comparative study, Int. J. Nucl. Desalin. 1 (2003) 30–46.
[5] Z. Ding, Analysis of a solar-powered membrane distillation system, Desalination 172 (2005) 27–40.
[6] S. Bouguecha, M. Dhahbi, Fluidised bed crystalliser and air gap membrane distillation as a solution to geothermal water desalination, Desalination 52 (2003) 237–244.
[7] M.S. El-Bourawi, Z. Ding, R. Ma, M. Khayet, A framework for better understanding membrane distillation separation process, J. Membr. Sci. 285 (2006) 4–29.
[8] A. Gabelman, S.T. Hwang, Hollow fiber membrane contactors, J. Membr. Sci. 159 (1999) 61–106.
[9] K.W. Lawson, D.R. Lloyd, Membrane distillation (review), J. Membr. Sci. 124 (1997) 1–25.
[10] E. Marsano, L. Francis, F. Giunco, Polyamide 6 nanofibrous nonwovens via electrospinning, J. App. Pol. Sci. 117 (2010) 1754–1765.
[11] L. Francis, J. Venugopal, M.P. Prabhakaran, V. Thavasi, E. Marsano, S. Ramakrishna, Simultaneous electrospin-electrosprayed biocomposite nanofibrous scaffolds for bone tissue regeneration, Acta Biomater. 6 (2010) 4100–4109.
[12] J.A. Matthews, G.E. Wnek, D.G. Simpson, G.L. Bowlin, Electrospinning of collagen nanofibers, Biomacromolecules 3 (2002) 232–238.

[13] C.Y. Xu, R. Inai, M. Kotaki, S. Ramakrishna, Aligned biodegradable nanofibrous structure: a potential scaffold for blood vessel engineering, Biomaterials 25 (2004) 877–886.
[14] L. Francis, A. Sreekumaran, R. Jose, S. Ramakrishna, V. Thavasi, E. Marsano, Fabrication and characterization of dye-sensitized solar cells from rutile nanofibers and nanorods, Energy 36 (2011) 627–632.
[15] C. Drew, X. Wang, K. Senecal, H. Schreuder-Gibson, J. He, J. Kumar, L.A. Samuelson, Electrospun photovoltaic cells, J. Macromol. Sci. A 39 (2002) 1085–1094.
[16] M.G. Hajra, K. Mehta, G.G. Chase, Effects of humidity, temperature, and nanofibers on drop coalescence in glass fiber media, Sep. Purif. Technol. 30 (2003) 79–88.
[17] P. Gibson, H. Schreuder-Gibson, D. Rivin, Transport properties of porous membranes based on electrospun nanofibers, Colloids Surf. A 187–188 (2001) 469–481.
[18] Z. Ma, M. Kotaki, S. Ramakrishna, Electrospun cellulose nanofiber as affinity membrane, J. Membr. Sci. 265 (2005) 115–123.
[19] X. Wang, C. Drew, S.H. Lee, K.J. Senecal, J. Kumar, L.A. Samuelson, Electrospun nanofibrous membranes for highly sensitive optical sensors, Nano Lett. 2 (2002) 1273–1275.
[20] X. Wang, Y.G. Kim, C. Drew, B.C. Ku, J. Kumar, L.A. Samuelson, Electrostatic assembly of conjugated polymer thin layers on electrospun nanofibrous membranes for biosensors, Nano Lett. 4 (2004) 331–334.
[21] M.M. Bergshoef, G.J. Vancso, Transparent nanocomposites with ultrathin, electrospun nylon-4,6 fiber reinforcement, Adv. Mater. 11 (1999) 1362–1365.
[22] J.S. Kim, D.H. Reneker, Mechanical properties of composites using ultrafine electrospun fibers, Polym. Compos. 20 (1999) 124–131.
[23] F. Lijo, E. Marsano, C. Vijila, R.S. Barhate, V.K. Vijay, S. Ramakrishna, V. Thavasi, Electrospun polyimide/titanium dioxide composite nanofibrous membrane by electrospinning and electrospraying, J. Nanosci. Nanotechnol. 11(2) (2011) 1154–1159.